

Superconductors for power applications: an executable and web application to learn about resistive fault current limiters

Nicolò Riva¹, Francesco Grilli², Bertrand Dutoit¹

¹École Polytechnique Fédérale de Lausanne, Switzerland

²Karlsruhe Institute of Technology, Germany

E-mail: nicolo.riva@epfl.ch

Abstract. High-temperature superconductors (HTS) can be superconducting in liquid nitrogen (77 K) at atmospheric pressure, which holds immense promises for our future such as nuclear fusion, compact medical devices and efficient power applications. In a power system, high short-circuit currents can exceed the operational current by more than ten times, putting at risk many parts of the system. Superconducting fault current limiters (SFCL) can limit the prospective fault current without disconnecting the power system, and are thus becoming increasingly attractive for future grids. With a growing interest in modeling and commercializing SFCL, the question of how to teach and to explain their operation to students has arisen. In order to help students visualize the potential use and benefits of a SFCL, we created an executable and a web application using COMSOL Multiphysics. This executable allows students to investigate the electro-thermal response of a resistive SFCL. The executable solves a 1-D electro-thermal model of the SFCL under AC fault conditions, evaluating important figures of merit such as the limited current, the prospective current and the maximum temperature reached within the tape. Finally, the geometrical parameters as well as the superconducting properties of the device can be modified. The importance of the amount of silver stabilizer necessary to protect the device from over-heating occurring during a fault current can be investigated. In addition, the effects of having a sharp nonlinear transition from the superconducting to the normal state (intrinsic property of the superconductor) to obtain a current limitation can be well explored. The executable allows the users to learn about the consequences of superconductors in real-life applications, without the prerequisite of extensive modeling or experimental setup. The executable can be downloaded from the HTS modeling website and run on the most commonly used operating systems.

[NOTE FOR THE REVIEWERS: The Comsol file and the executable can be found with the submitted material. They will be later available on [1]. The web version of the executable can be found at [2].

1. Introduction

Given the ever increasing role of electricity in our society, protecting electric grids from faults and surges has become of paramount importance. For this purpose, different

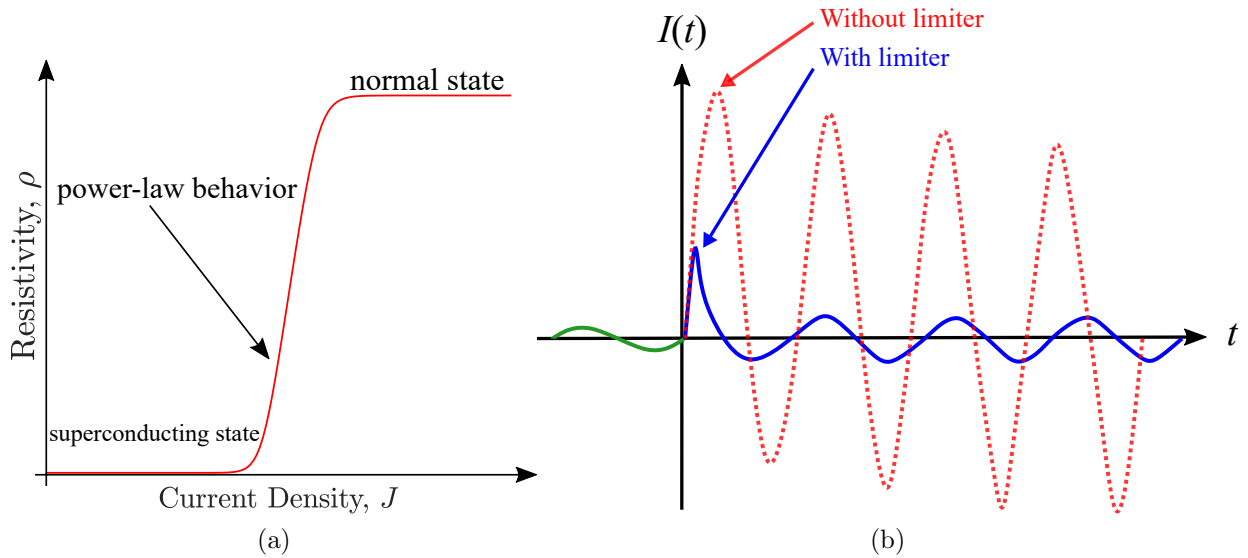


Figure 1: (a) Non-linear dependence of the superconductor’s resistivity on the current density and (b) schematic representation of what occurs to the current flowing in the grid during a fault if a current limiter is present or not.

technologies have been developed: these include explosive I_s -limiters, high-voltage fuses and air-core reactors. These technologies, while effective, present important limitations, for example added circuit impedance during normal operation, limited scalability, and high maintenance efforts [3]. The disruptive technology offered by superconductivity allows overcoming these limitations. Superconducting fault current limiters (SFCL) are devices that are essentially ‘transparent’ during normal operation (with no or very limited energy dissipation) and that present a huge and rapid increase of their resistance during a fault. In *resistive* SFCL, this behavior resides in the intrinsic physical behavior of the superconducting material, i.e. in an extremely non-linear dependence of the resistance on the current flowing through the device (figure 1).[‡] During normal operation, the superconductor operates in the zero-resistivity region represented in figure 1a, where it has no (in direct current regime) or very low (in alternating current regime) losses.[§] During a fault, the resistivity of the superconductor increases rapidly to extremely high values, i.e. $100 \mu\Omega \text{ cm}$ in the normal-state (figure 1a): this increase of the material’s resistivity can be used to limit the current flowing in the electric circuit, thus protecting the load. Figure 1b represents what occurs to the current flowing in the grid during a fault if a current limiter is present (continuous blue line) or not (red

[‡] Other types of SFCL exist, for example bridge-type and shielded iron core fault SFCL. In those cases, the nonlinear behavior is given by the power electronics and by the magnetic materials, respectively. Superconducting tapes are used instead of normal conducting coils in order to reduce the size of the device, but not directly as current limiting materials. See [3] for details and examples. In this article we consider only resistive SFCL.

[§] An introduction to the topic of AC losses in superconductor, which includes a numerical model implemented in an open-source finite-element program, can be found in [4].

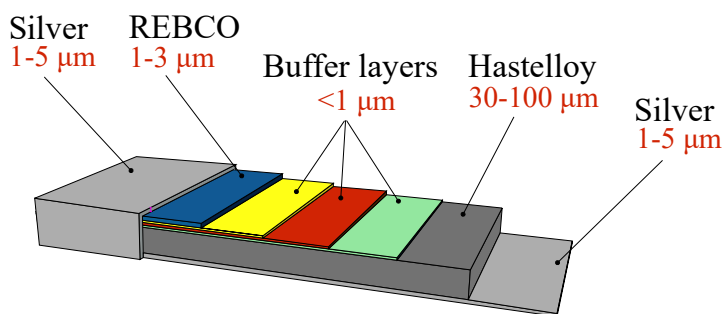


Figure 2: Typical structure of a REBCO commercial tape (representation not to scale).

dashed line). Without a current limiter, the large current oscillations resulting from the fault put the grid equipment at risk. The ultimate effect of a non-limited fault is an economic damage for both the operator and the customer. High-temperature superconductors (HTS), with critical temperatures well above the boiling temperature of liquid nitrogen at atmospheric pressure (77 K), are particularly indicated for SFCL applications: compared to classical low-temperature superconductors, they have lower refrigeration costs and increased heat capacity. Currently, the most promising HTS are manufactured in the forms of multi-layer tapes, where the superconductor material is a thin film, only a few micrometers thick. Additional copper layers provide electrical and thermal stabilization. The superconducting material has the chemical formula (RE)Ba₂Cu₃O₇, where RE indicates a rare earth element. They are often indicated as REBCO coated conductors and their typical structure is shown in figure 2.

The performance of coated conductors in SFCL dramatically depends on their structure (e.g. the thickness of the different layers), on the physical properties of the superconductor material, and on the cooling conditions. Researchers around the world are trying to optimize REBCO coated conductors for SFCL applications [5, 6, 7, 8].

The aim of this work is to introduce the readers to the use of REBCO coated conductors for SFCL application, with particular focus on the role of the tape's structure and physical parameters on the current limiting behavior. For this purpose, we developed a finite-element model for the electro-thermal behavior of the tape in fault-current limiting applications. The model is implemented in the COMSOL Multiphysics environment and distributed as a COMSOL application, as an executable [1], and as a web application within the project AURORA (learning superconductivity through apps) [2].

With a simulation application, complex concepts can be incorporated behind a user-friendly interface, so that users do not have to deal with unnecessary jargon. In addition, this type of applications enables an easy access to simulation tools that can generate interest in students and provide values to companies.

2. Superconducting fault current limiters

In resistive SFCL, after transition, the superconducting tape needs to absorb and spread the energy during the limitation phase. Ideally, the transition from the superconducting to the normal state occurs uniformly along the tape's length. The energy balance can be written as follows:

$$L_{\text{tape}} \int_0^{t_{\text{lim}}} E(I, T) I(t) dt = \int_0^{t_{\text{lim}}} m C_p(T) \cdot (T - T_0) dt + Q_{\text{bath}}, \quad (1)$$

where the dissipated energy (left hand side) is either absorbed by the wire (right hand side, first term) or exchanged with the cryogenic bath (right hand side, second term). In equation (1), L_{tape} is the tape's length, t_{lim} is the time duration of the limitation, $E(I, T)$ is the electric field (which depends on the current I and on the temperature T), m is the tape's mass, C_p is the tape's heat capacity, and T_0 is the starting operating temperature.||

In the analysis presented in equation (1), we introduce a few simplifications. If the quench is sufficiently fast, the energy exchange with the bath is low: we are close to adiabatic conditions and the term Q_{bath} is negligible. In addition, for a clear fault, i.e. $I \gg I_c$, E does not depend on I anymore because the current flows only in the stabilizer and in the substrate. In order to avoid permanent damage to the superconducting tape, the final temperature $T(t_{\text{lim}})$ has to be under a threshold, generally from 400 K to 450 K for coated conductors. Then, for a given limitation time, the main structural parameter around which the construction of the device can be adjusted is the mass of the conductor, which can be increased by making the tape thicker and/or longer. The generated heat must be sufficiently uniform and the conductor's length kept within reasonable limits for economic reasons. The mass can be increased by making the tape thicker and/or longer.

The electric field E is a parameter characterizing the device: 50 V m⁻¹ is a typical value for a tape with a 100 μm-thick substrate. A higher mass per unit length obtained by using a thicker substrate or even by adding high $C_p(T)$ material tightly thermally connected to the conductor will result in a higher electric field, up to 200 V m⁻¹. Higher electric fields can be obtained by using sapphire-based substrates [10]: their very high thermal conductivity would allow a millimeter-thick substrate without significant thermal gradient on the cross section.

In resistive SFCL, the superconducting tape needs to be sufficiently long in order to absorb and spread the energy during limitation. In order to limit the size of the device, the tape is wound in the form of pancake coils, with a bifilar design (figure 3a),

|| A less ideal situation is represented by high-impedance faults, with the current I close to I_c . In such cases, the non-homogeneity of the critical current along the conductor leads to localized transitions to normal state and to the formations of the so-called *hot spots*. The same energy balance given by equation (1) applies locally and t_{lim} has still to be short enough. In practice, it is quite difficult to detect the hot spots early enough to maintain t_{lim} short and thus keep the local temperature at safe value. A high normal zone propagation velocity (NZPV) is helpful to protect against hot spots [9].

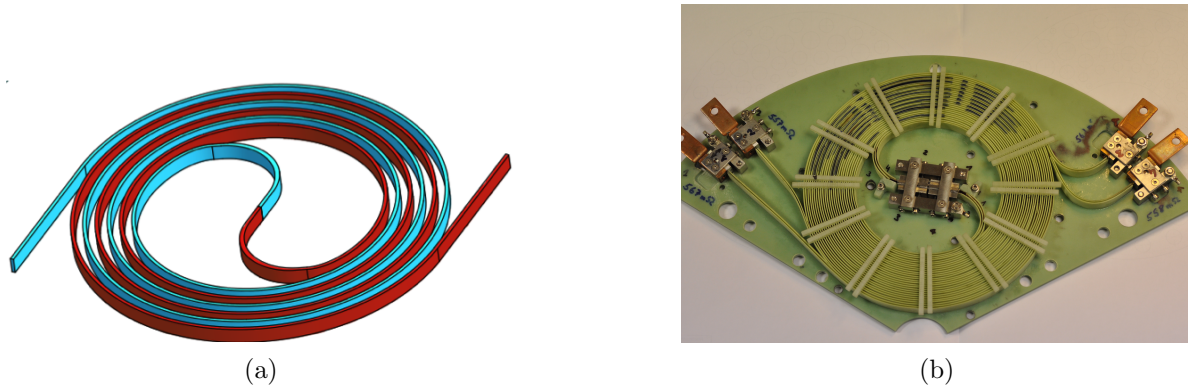


Figure 3: Bifilar coils for SFCL application: schematic illustration and picture of the module used in the Ensystrob project [12] .

where the current of adjacent turns flows in opposite direction. This greatly reduces the coil's impedance and, thanks to the suppression of the magnetic field component perpendicular to the flat face of the tape, the AC losses as well [11]. A picture of the bifilar coil module used in the Ensystrob project [12] is shown in figure 3b.

3. COMSOL model of HTS wire for fault current limiter applications

In this section we describe the model implemented using the commercial software COMSOL Multiphysics [13]. A similar model was developed from the authors in [14].

3.1. Heat equation in 1-D coupled with equivalent circuit model

The model is a 1-D thermal finite-element model (temperature variation across the thickness of the tape) coupled with an electric circuit model (current sharing between the various layers of the tape). We assume that the tape's electrical and thermal properties do not vary significantly along the tape's width and length. The equivalent 1-D electrical model of the SFCL is represented in figure 4.

The SFCL is modeled as a set of resistors in parallel, representing the stabilizer (in this case silver), the Hastelloy and the REBCO layers, respectively. Each resistor $R_i(I_i, T_i)$ is defined by the electrical resistivity $\rho_{el,i}(I_i, T_i)$, the length of the the tape L_{tape} , its width w_{tape} and the thickness of the single layer h_i , where the subscript i identifies the layer of the tape (i.e. silver, REBCO, etc.). A voltage V_{app} or a current I_{app} can be applied between the tape terminals A and B . The heat equation, modeled in the Heat Transfer Module (ht) of COMSOL Multiphysics, is coupled with the equivalent circuit model of the SFCL, modeled in the Electric Circuit Module (cir) [13]. The heat equation is solved in each 1-D domain, schematically represented in figure 4, and reads as follows:

$$\rho_{\text{mass},i}(T_i)C_{p,i}(T_i)\frac{\partial T_i}{\partial t} + \frac{\partial}{\partial x} \left(-k_i(T_i)\frac{\partial T_i}{\partial x} \right) = \frac{R_i(I_i, T_i) \cdot I_i^2}{\Omega_i} - h_{\text{LN}_2} \cdot (T_i - T_0) \Big|_{\partial\Omega}, \quad (2)$$

where on the left side we have the mass density $\rho_{\text{mass},i}(T_i)$, the specific heat capacity $C_{p,i}(T_i)$ and the thermal conductivity $k_i(T_i)$. On the right side of equation, there is the heat source term and a cooling term. The heat source comes from Joule's first law, i.e. $P = R_i \cdot I_i^2 / \Omega_i$, and the volume of the conductor is noted as $\Omega_i = w_{\text{tape}} \cdot L_{\text{tape}} \cdot h_i$. The heat exchange with the liquid nitrogen is taken into account by applying a boundary condition applied only on the top and the bottom layers of the tape (silver surfaces), indicated by $\partial\Omega$. In equation (2), the heat transfer coefficient $h_{\text{LN}_2}(T_i - T_0)$ is a function of the temperature [15]. For better readability, the temperature dependence of $h_{\text{LN}_2}(T_i - T_0)$ is omitted and the transfer coefficient is simply written as h_{LN_2} . The temperature dependence of all the thermal and electrical material properties is taken into account. For R_{REBCO} , we consider the power-law model with a temperature-dependent critical current $I_c(T)$. We write the power-law as follows:

$$\rho_{\text{PLW}}^{\text{SC}}(I, T) = \frac{\Sigma \cdot E_c}{I_c(T)} \left(\frac{|I|}{I_c(T)} \right)^{n-1}, \quad (3)$$

where Σ is the cross section of the REBCO layer, $E_c = 1 \mu\text{V cm}^{-1}$ is the electric field criterion and n is the constant power-law exponent, and $I_c(T)$ is given by a relationship of the form:

$$I_c(T) = I_{c,77\text{K}} \cdot \frac{T_c - T}{T_c - 77\text{K}}. \quad (4)$$

The normal state resistivity $\rho_{\text{NS}}(T)$ of REBCO is added in parallel to the power-law, in order to obtain a total resistivity that better reproduces the electrical behavior of REBCO [16] over a wide current and temperature range, i.e.:

$$\rho_{\text{PLW}} = \frac{\rho_{\text{PLW}}^{\text{SC}}(I, T) \cdot \rho_{\text{NS}}(T)}{\rho_{\text{PLW}}^{\text{SC}}(I, T) + \rho_{\text{NS}}(T)}. \quad (5)$$

The temperature dependence of the normal-state resistivity of REBCO is modeled with a simple linear relationship [17], i.e.:

$$\rho_{\text{NS}}(T) = \rho_{T_c} + \alpha \cdot (T - T_c),$$

where $\rho_{T_c} = 100 \mu\Omega \text{ cm}$ and $\alpha = 0.47 \mu\Omega \text{ cm K}^{-1}$ [18].

The complete circuit model used to simulate AC fault current limitation is presented in figure 4. A sinusoidal voltage signal is imposed on the circuit, while a load resistor R_{Load} draws the nominal current from the source. A switch in parallel to the load resistor, when closed, simulates the fault occurring at a given time and draws the fault current through a resistor R_{fault} . In the simulations, V_{peak} can be changed and $f = 50 \text{ Hz}$ is fixed. The switch operates at $t = 20 \text{ ms}$ and the short-circuit is cleared after two periods of the sinusoidal voltage source, i.e. $t = 60 \text{ ms}$. Finally, the prospective current is calculated as $I_{\text{fault}} = V_{\text{peak}} / R_{\text{fault}}$.

3.2. Heat equation in 1-D to estimate the cooling temperature profile

Another interesting aspect is the temperature cooling profile of the tape. Once the superconducting tape has recovered from the fault, the nominal operation of the grid

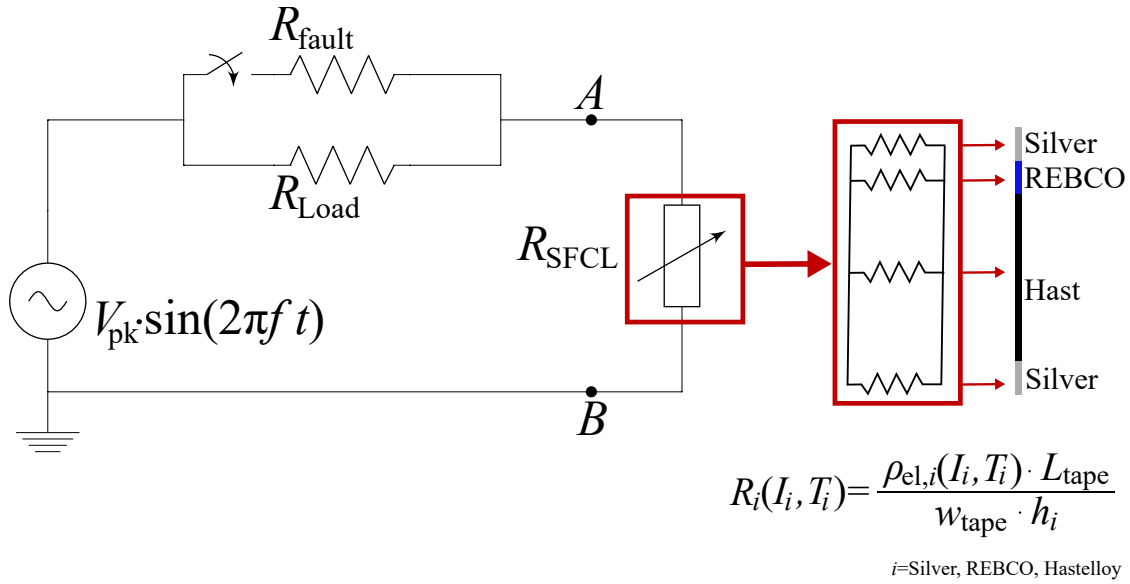


Figure 4: Schematic circuit representing the electric circuit model, and representation of the REBCO tape implemented in COMSOL.

must be reestablished. This means that the SFCL must also be invisible to the grid (negligible impedance) and thus in the superconducting state. This condition implies that the temperature of the SFCL, especially the REBCO layer, must be below its critical temperature T_c , which is around 92 K [19].

The complex non-linear heat transfer coefficient of the liquid nitrogen does not allow to estimate the cooling-temperature profile of the SFCL analytically, and thus, its recovery time. As a consequence, these quantities are estimated with numerical methods.

The time-scale at which the fault occurs (tents of ms) is very different from that of cooling, which is typically around hundreds of ms or s. The numerical solution of phenomena occurring at very different time-scales can lead to long computational times. This is undesired, especially when the user expects the simulation to run in a few minutes, as in the case of a student during a lecture. To address this issue, one can note that during the cooling of the tape the only physics involved is the heat transfer between layers and liquid nitrogen. As a consequence, we can neglect the circuitual part and study the temperature profile of the tape with a second model. The second model uses the temperature profile of the tape at the end of the first simulation as initial condition, and the initial time of the second model is the final one of the first model $t_0 = t_{\text{fin}}$. As a consequence we have:

$$T(t_0)^{\text{2nd-model}}(x) = T(t_{\text{fin}})^{\text{1st-model}}(x). \quad (6)$$

The second model solves the heat equation on the same domains, but for a longer time (i.e., 2s) and with a larger time step. This ensures the simulation of a time sufficiently long to observe the temperature cooling profile while having a short computational time.

The computing time of the first model (fault over 100 ms) ranges from 30 s to 40 s per run, while the computing time of the second model (tape cooling from 100 ms to 2 s) ranges from 6 s to 10 s per run. Once the simulation is run, the solver is concatenated and the overall simulation takes from 35 s to 60 s run. These computing times were obtained by running the executable on an Intel(R) Core(TM) i5-7Y57 CPU @ 1.30 GHz).

Since the main design criteria are to avoid burning the tape, we need to know whether this happened after the fault. At the end of the simulation, a dialog box informs about the status of the tape. Specifically, the box informs if the tape reached more than 450 K and if, after 2 s¶, the tape recovered, and its temperature is below 92 K. The maximum temperature displayed in the box is obtained by calculating the average temperature profile on the 1-D REBCO domain and selecting the maximum value of this curve.

3.3. User interface and parameter calibration

In figure 5 we present the user interface. In the upper part (black-dashed box), we have the dashboard where we can find the functional buttons of the executable. Besides running the simulations (“*Compute*”) and plotting the results (“*Plot*”), it is possible to consult a presentation describing some relevant test cases (“*Slide/Paper*”) and also to export the results in form of report (*.html/.doc*). The parameters that can be changed, and some figure of merits are indicated in figure 5.

In the *Circuit* drop-down list, the parameters that can be varied are V_{pk} , I_{nom} and $Ratio = R_{Load}/R_{fault}$. By selecting V_{pk} , one fixes the applied electric field E_{app} , since both the length of the tape ($l_{tape} = 200$ m), as well as its width ($w_{tape} = 12$ mm), are fixed by design. By choosing I_{nom} , one selects the nominal current flowing in the circuit in normal conditions. The critical current of the tape I_c (at 77 K and self-field conditions) is fixed accordingly, and arbitrarily, as $I_c = 1.2 I_{nom}$. Finally, by selecting the ratio between the nominal and fault impedance, one selects the prospective current as $I_{prosp} = Ratio \cdot I_{nom}$. At this point the user should select the tape parameters in the *Tape* drop-down list. The parameters that can be changed, in this case, are the n -value, the silver thickness h_{Ag} and the Hastelloy thickness h_{Hast} .

Once the parameters are set and the simulation is finished, the user can consult some merit figure such as the maximum temperature of the REBCO, the maximum limited current, and the prospective current (yellow-dashed box). Finally, the user can browse through the plots that report the quantities calculated from the model, such as the *Limiting current - Temperature* of the REBCO, the *Limiting current - Prospective current*, and the *Temperature cooling profile over 2 s* (green-dashed box).

¶ The choice of the cooling time is arbitrary. Usually, the devices need to be reconnected to the grid very quickly [3, 7]

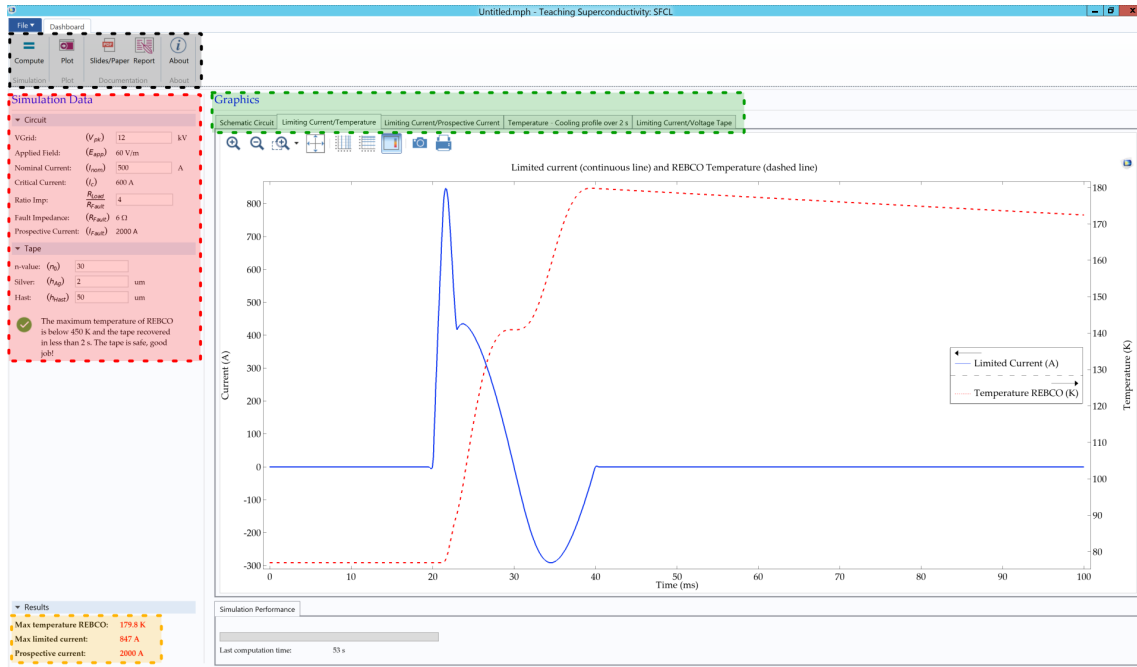


Figure 5: Screenshot of the executable. A description of the various parts is given in the text.

4. Results

In this section we present four cases obtained by varying the parameters described above. We selected four case scenario to highlight the importance of a sharp nonlinear transition, as well as the role played by the amount of stabilizer and Hastelloy. The parameters (referring to figure 4 and figure 5) are V_{pk} , I_{nom} , $Ratio$ and n_0 , h_{Ag} , h_{Hast} .

The user should tweak the parameters to asses how the output results change with respect to a given quantity. For instance, what does it happen if the n -value, which defines the strong non-linearity of the superconductor, is reduced?

4.1. Default parameters

The first case investigates the default parameter setting, namely:

- $V_{pk} = 12 \text{ kV}$ ($E_{app} = 60 \text{ V m}^{-1}$)
- $I_{nom} = 500 \text{ A}$ ($I_c = 600 \text{ A}$)
- $Ratio = 4$ ($I_{prosp} = 2000 \text{ A}$)
- $n_0 = 30$
- $h_{Ag} = 2 \text{ } \mu\text{m}$
- $h_{Hast} = 50 \text{ } \mu\text{m}$.

As shown in figure 6(a-b-c), with these parameters the tape is safe: the temperature stays below 450 K for the entire duration of the fault, and the limited current ($< 1000 \text{ A}$)

is smaller than the prospective one (2000 A).

4.2. Small n -value (low non-linear behavior)

In the second case all the parameters are kept as in the first case, except for the n -value. In this case the n -value is very small (i.e., $n = 5$) with respect to the commonly n -values of REBCO tapes (i.e., $n \approx 30$ [20]). The superconductor has a smoother transition to the normal state and its behavior is closer to that of an ohmic material ($n = 1$).

The results (figure 6(d-e-f)) show that, for $n = 5$, the current flowing in the system is overlapped to the prospective current, and thus, the current is not limited (figure 6(d)). The simulated temperature profile in the REBCO predicts a very small temperature increase ($\Delta T \approx 0.4$ K). This means that the REBCO tape is still safe; however it is possible that other parts of the system, sensitive to overcurrents, are permanently damaged.

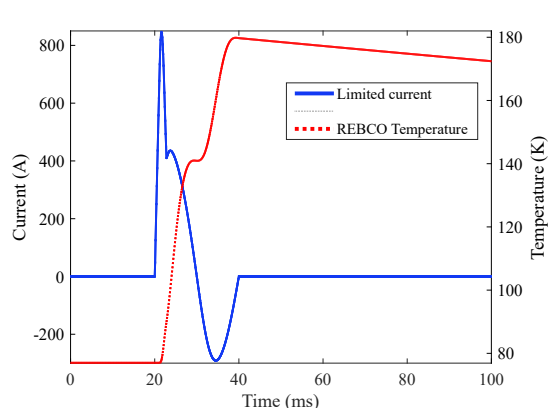
This case highlights the crucial role played by the high non-linearity of the superconductor in making the current limitation effective.

4.3. Low impedance fault, higher applied electric field, and thin Hastelloy layer

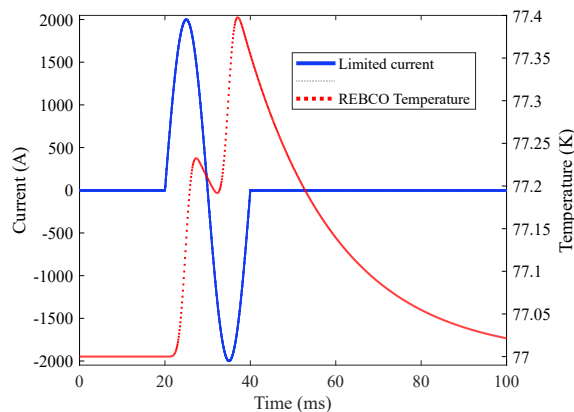
The third case investigates a more realistic situation, where the prospective fault current can reach to 10-12 times the critical current, and the applied electric field is higher. All the parameters are kept as in the first case except for $V_{pk} = 40$ kV ($E_{app} = 200$ V m⁻¹) and $Ratio = 10$ ($I_{prosp} = 5000$ A). The results in figure 7(a-b-c) show that the limited current (< 1000 A) is smaller than the prospective one (5000 A). However, the REBCO tape is burnt since the temperature goes above 450 K. A possible solution is to add mass to the tape. This can be done by increasing the thickness of the Hastelloy layer.

4.4. Low impedance fault, higher applied electric field, and thick Hastelloy layer

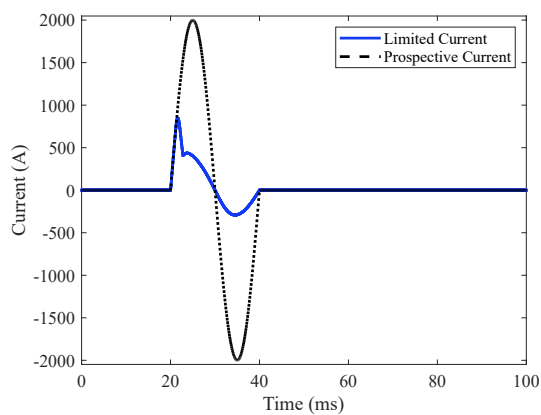
In the last case scenario we keep the same circuit parameters of the previous case, but we increase up to 100 μ m the thickness of the Hastelloy layer. The results are presented in figure 7(d-e-f). The electrical quantities (voltage and current) are the same, while the simulated temperature in the REBCO is substantially decreased and is below 450 K.



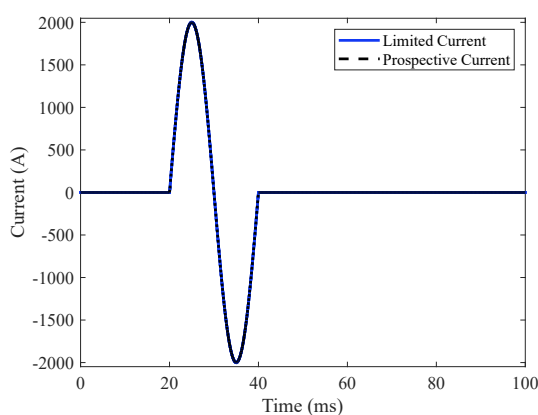
(a) Limited current/Temperature REBCO (Default parameters)



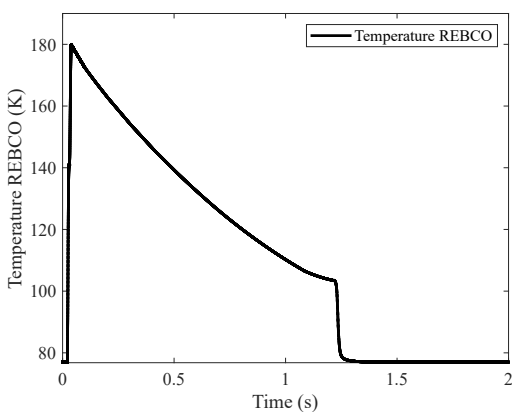
(d) Limited current/Temperature REBCO (Small n -value)



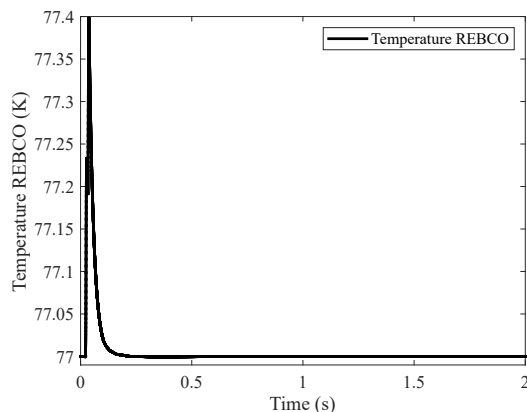
(b) Limited and prospective current (Default parameters)



(e) Limited and prospective current (Small n -value)

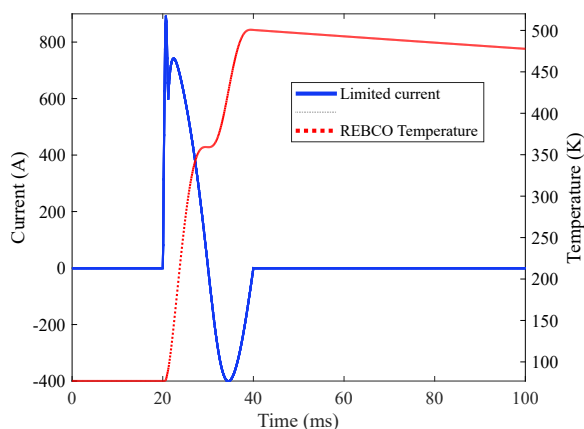


(c) Cooling temperature profile REBCO (Default parameters)

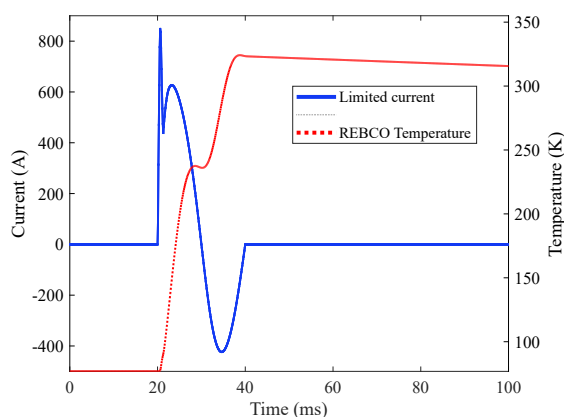


(f) Cooling temperature profile REBCO (Small n -value)

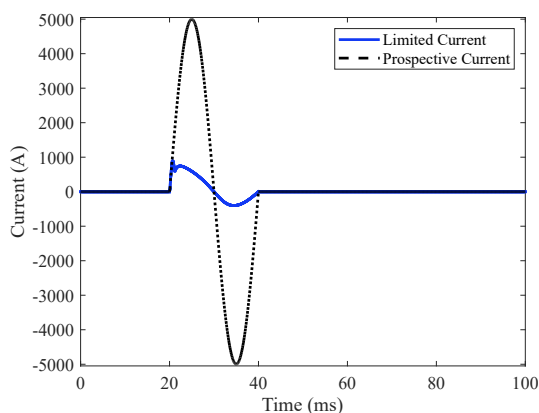
Figure 6: Simulation results using (left) the default parameters and (right) a small n -value.



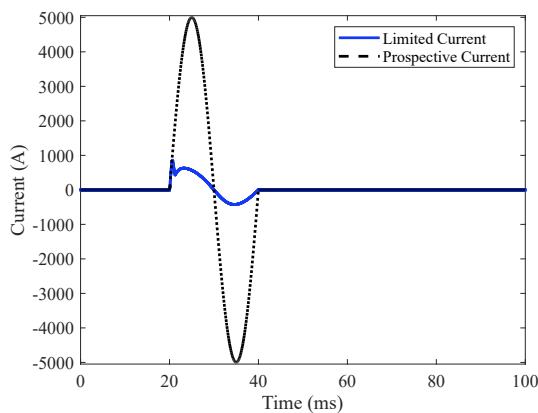
(a) Limited current/Temperature REBCO High fault - thin Hastelloy



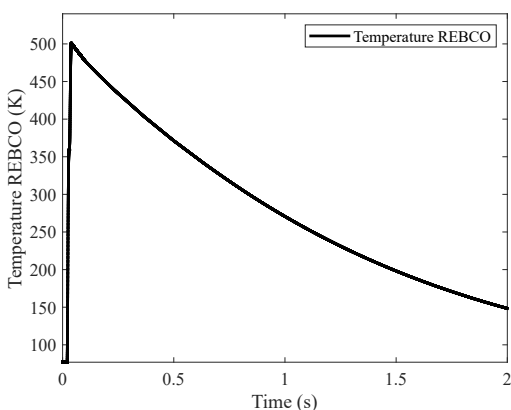
(d) Limited current/Temperature REBCO High fault - thick Hastelloy



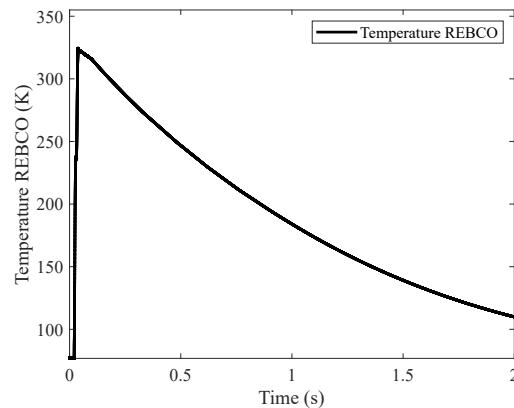
(b) Limited and prospective current High fault - thin Hastelloy



(e) Limited and prospective current High fault - thick Hastelloy



(c) Cooling temperature profile REBCO High fault - thin Hastelloy



(f) Cooling temperature profile REBCO High fault - thick Hastelloy

Figure 7: Simulation results for a high prospective current fault with a (left) thin and (right) thick Hastelloy layer.

5. Conclusion

In this paper we presented an executable that can be used to introduce students to the benefits of using superconductors in power applications, specifically a resistive SFCL. The executable solves a 1-D electro-thermal model of the SFCL under AC fault conditions. With this tool, students can learn about the influence of circuit and tape parameters on the electro-thermal of a SFCL. We presented four case scenario to highlight the importance of a sharp nonlinear transition, as well as the role played by the amount of Hastelloy. The students however, can quickly simulate different cases since the running time is relatively short (tents of seconds). The model is developed in COMSOL Multiphysics and is deployed in various forms, including executable files (running on the most common operating systems) [1] and as web application within the project AURORA (learning superconductivity through apps) [2].

References

- [1] HTS Modelling Workgroup URL <http://www.htsmodelling.com/>
- [2] AURORA - Learning superconductivity through apps URL <https://aurora.epfl.ch/app-lib>
- [3] Noe M and Steurer M 2007 *Superconductor Science and Technology* **20** R15–R29 URL <https://doi.org/10.1088/0953-2048/20/3/R01>
- [4] Grilli F and Rizzo E 2020 *European Journal of Physics* **41** 045203 URL <https://doi.org/10.1088/1361-6404/ab90dc>
- [5] Ruiz H, Zhong Z and Coombs T 2015 *IEEE Transactions on Applied Superconductivity* **25** 5601405 URL <http://doi.org/10.1109/TASC.2014.2387115>
- [6] Tixador P 2018 *Superconducting Fault Current Limiter* (World Scientific) (Preprint <https://www.worldscientific.com/doi/pdf/10.1142/11062>) URL <https://doi.org/10.1142/11062>
- [7] Tixador P, Bauer M, Bruzek C, Calleja A, Deutscher G, Dutoit B, Gomory F, Martini L, Noe M, Obradors X, Pekarčíková M and Sirois F 2019 *IEEE Transactions on Applied Superconductivity* **29** 5603305 URL <https://doi.org/10.1109/TASC.2019.2908586>
- [8] Bock J, Bludau M, Schramm J, Krämer S, Jänke C, Rikel M and Elschner S 2011 21 st International Conference on Electricity Distribution Paper 0352 NEXANS 'Superconducting fault current limiters for medium voltage applications – STATUS AND PROSPECTS 21 st International Conference on Electricity Distribution Tech. Rep. 0352 URL <https://www.researchgate.net/project/Superconducting-FCL>
- [9] Deutscher G 2018 *Journal of Superconductivity and Novel Magnetism* **31** 1961–1963 URL <https://doi.org/10.1007/s10948-018-4633-8>
- [10] Lacroix C and Sirois F 2014 *Superconductor Science and Technology* **27** 035003 URL <https://doi.org/10.1088/0953-2048/27/3/035003>
- [11] Clem J R 2008 *Physical Review B* **77** 134506 URL <https://doi.org/10.1103/PhysRevB.77.134506>
- [12] Elschner S, Kudymow A, Brand J, Fink S, Goldacker W, Grilli F, Noe M, Vojenciak M, Hobl A, Bludau M, Jänke C, Krämer S and Bock J 2012 *Physica C* **482** 98–104 URL <https://doi.org/10.1016/j.physc.2012.04.025>
- [13] Finite-element software package Comsol Multiphysics. <http://www.comsol.com>
- [14] Riva N, Sirois F, Lacroix C, de Sousa W T B, Dutoit B and Grilli F 2020 *Superconductor Science and Technology* **33** 114008 URL <https://iopscience.iop.org/article/10.1088/1361-6668/aba34e>
- [15] Roy F 2010 *Modeling and Characterization of Coated Conductors Applied to the Design of*

- Superconducting Fault Current Limiters* Ph.D. thesis École Polytechnique Fédérale de Lausanne
<https://infoscience.epfl.ch/record/148348>
- [16] Duron J, Grilli F, Dutoit B and Stavrev S 2004 *Physica C* **401** 231–235 URL <http://doi.org/10.1016/j.physc.2003.09.044>
- [17] Bonnard C H, Sirois F, Lacroix C and Didier G 2017 *Superconductor Science and Technology* **30** 014005 URL <https://doi.org/10.1088/0953-2048/30/1/014005>
- [18] Friedmann T A, Rabin M W, Giapintzakis J, Rice J P and Ginsberg D M 1990 *Phys. Rev. B* **42** 6217–6221 URL <https://doi.org/10.1103/PhysRevB.42.6217>
- [19] Wu M K, Ashburn J R, Torng C J, Hor P H, Meng R L, Gao L, Huang Z J, Wang Y Q and Chu C W 1987 *Physical Review Letters* **58** 908–910 URL <https://doi.org/10.1103/PhysRevLett.58.908>
- [20] Ainslie M D, Bumby C W, Jiang Z, Toyomoto R and Amemiya N 2018 *Superconductor Science and Technology* **31** 074003 URL <https://doi.org/10.1088/1361-6668/aac1d3>